Anonymous Referee #3

This study proposes a novel methodology based on Longitudinal Wave Power (LWP) to identify coastal morphological changes, aiming to improve upon traditional approaches that rely solely on wave height (Hs). Through numerical simulations, the research demonstrates that the LWP-based method outperforms the Hs-based approach. The work is innovative and holds potential for coastal management applications. However, several details require further discussion and clarification. The following suggestions are provided to strengthen the manuscript:

The authors sincerely thank Reviewer 3 for their careful reading and insightful comments on our manuscript. Following their guidance, we have significantly revised the manuscript and added a new section regarding its application to real-world scenarios. To address the concerns about the absence of field data, we have now implemented the methodology using real-world models of two different study areas along the South Atlantic coast of the Iberian Peninsula. These applications were carried out using previously calibrated and validated numerical models, whose calibration and validation were performed against real measured bathymetric data. This provides a meaningful empirical grounding for the methodology beyond the idealized framework, while also introducing real-world forcings including observed wave conditions, complete tidal regimes, and variable river discharges, and also different sediment grain sizes.

1. **The study is based on idealized numerical simulations; however, the differences between an idealized coastal zone and real-world, complex topography are not discussed. Furthermore, the use of only six wave climate conditions may not adequately capture natural variability. It is necessary to discuss how these simplifications affect the generalizability of the conclusions. The authors could consider supplementing the analysis with additional climate scenarios or case studies for validation.**

Following the reviewers' suggestions, a new section has been incorporated into the manuscript to present the application of the methodology to two real-world study areas. These applications were carried out using previously calibrated and validated numerical models, whose calibration and validation were performed against real measured bathymetric data. This provides a meaningful empirical grounding for the methodology beyond the idealized framework, while also introducing real-world forcings including observed wave conditions, complete tidal regimes, and variable river discharges, and also different sediment grain sizes. As shown in the revised manuscript, the new Section 5, "Application to real-world study areas", reads as follows:

"*The methodology was applied to two different real-world study areas: the Punta Umbría Inlet, following Zarzuelo et al. (2019) and the Guadiana estuary, following López-Ruiz et al. (2020). For both study cases, models were implemented in Delft3D and have been calibrated and validated against field-measured bathymetric surveys, providing continuous morphological simulations over real observed periods. For the Punta Umbría Inlet, the model spans from July 2014 to October 2015, with model data obtained at 3-hour intervals. For the Guadiana estuary, two separate simulations with hourly data were utilized: (1) from July 2016 to June 2017, and (2) from June 2017 to December 2018. This section presents the match results for each simulation using the two primary POT combinations: T-POT and Combination 11.*

5.1. Punta Umbría Inlet

The Punta Umbría Inlet (hereinafter PUI) consists of a NW-SE trending channel, 8 km in length and 0.5 km in width, with a maximum depth of -12 m MSL. Characterized as an ebb-tidal system, it features minor ebb channels, shoals, and frontal lobes. The model utilizes a spatially distributed D_{50} sediment grain size, ranging from 0.5 to 4 mm. This is defined via a grid-based input file to reflect the natural variability of the seabed. Due to long-standing navigational difficulties associated with shoal development, a jetty was constructed at the inlet, reaching -4 m MSL. The numerical setup and validation procedures follow Zarzuelo et al. (2019) in their entirety. A comprehensive description of the model performance is available in that study.

The control volume used to apply the methodology is located in the channel (Figure S11 from Supplementary Material). The match values obtained for the T-POT are 43.4% and 41.4% for the LWP-ME90 and LWP-ME95, respectively, and 42,7% and 45,1% for the H_s-ME90 and H_s-ME95, respectively. For the optimal combination (Combination 11, POT(95,4,6)), the match results for LWP increase to 47.4% (ME90) and 47.5% (ME95), while the H_s matches remain identical to those of the T-POT. This suggests that the optimal POT combination improves upon the T-POT for LWP while maintaining the same accuracy for H_s.

5.2. Guadiana estuary

The numerical setup for the Guadiana estuary follows the configuration described in López-Ruiz et al. (2020), where a comprehensive description of the model's calibration and performance is available. The study area encompasses the ebb-tidal delta of the Guadiana River, located at the southern border between Spain and Portugal. The region is characterized by a semi-diurnal mesotidal regime, with a mean tidal range of 2 m. Similar to the PUI, the river mouth is stabilized by a jetty system, and the main channel undergoes periodic dredging to maintain navigability. Sediment distribution in the area exhibits the high variability typical of deltaic environments, with grain sizes ranging from fine to coarse sands. The model utilizes a spatially distributed D_{50} sediment grain size, ranging from 1 to 10 mm. This is defined via a grid-based input file to reflect the natural variability of the seabed.

Two simulations covering different periods are available for this study area, hereafter referred to as Guadiana 1617 (from July 2016 to June 2017) and Guadiana 1718 (from June 2017 to December 2018). The control volume used to apply the methodology is located in the ebb delta, within an area comparable to the one analyzed by Garel et al. (2019) to unravel the sediment transport patterns in the delta (Figure S12 from Supplementary Material).

For Guadiana 1617, the match values obtained for the T-POT are 63.5% and 62.9% for the LWP-ME90 and LWP-ME95, respectively, and 64.3% and 63.9% for the H_s-ME90 and H_s-ME95, respectively. For the optimal combination (Combination 11, POT(95,4,6)), the match results for LWP increase to 67.5% (ME90) and 67.9% (ME95), while the H_s matches remain identical to those of the T-POT.

For the Guadiana 1718 period, the T-POT achieved match values of 72.3% and 90.5% for LWP (ME90 and ME95, respectively), and 73.1% and 90.5% for H_s. The optimal POT combination (Combination 11) improved the LWP-ME90 match to 79% and the H_s-ME90 to 74.4%, while maintaining identical results for all ME95 events. Notably, almost all ME95 morphological events occurred during Storm

Emma (February 2018), which heavily impacted the South Atlantic coast of the Iberian Peninsula (Málvarez et al. 2021).”

As demonstrated, the application to real-world scenarios confirms the robustness of the methodology. The optimal POT combination (Combination 11) consistently outperforms the T-POT across the three simulations analyzed regarding LWP matches. The single exception is the Guadiana 1718 case, where the dominance of a single extreme event (Storm Emma) concentrates nearly all ME95 events within a brief period, thereby limiting the discriminatory capacity of the LWP-based proxy under such specific conditions. This behavior is consistent with the role of the LvC index discussed in Section 6.1 of the revised manuscript (and further detailed in our response to Comment 1), reinforcing the complementary nature of LWP and Hs as morphological proxies. Moreover, the Hs related matches for the optimal POT combination are equal to the T-POT matches, with the exception of Guadiana 1718, where the match for Hs-ME90 shows an improvement over the T-POT.

Storm Emma (February 28 – March 5, 2018) was a severe Atlantic event that triggered extreme meteorological and oceanographic conditions across the southwestern Iberian Peninsula. It produced a 22-year record significant wave height of 7.27 m and raised sea levels to 4.12 m through a combination of low atmospheric pressure and spring tides. These forces caused profound morphodynamic changes, including dune erosion of 2.5 m and the modification of seabed elevation at depths as great as -10 m (García-de-Lomas, et al., 2019; Málvarez et al. 2021).

The Figures S11 and S12 from the Supplementary Material correspond to Figure 1 and Figure 2, respectively, from the present document.

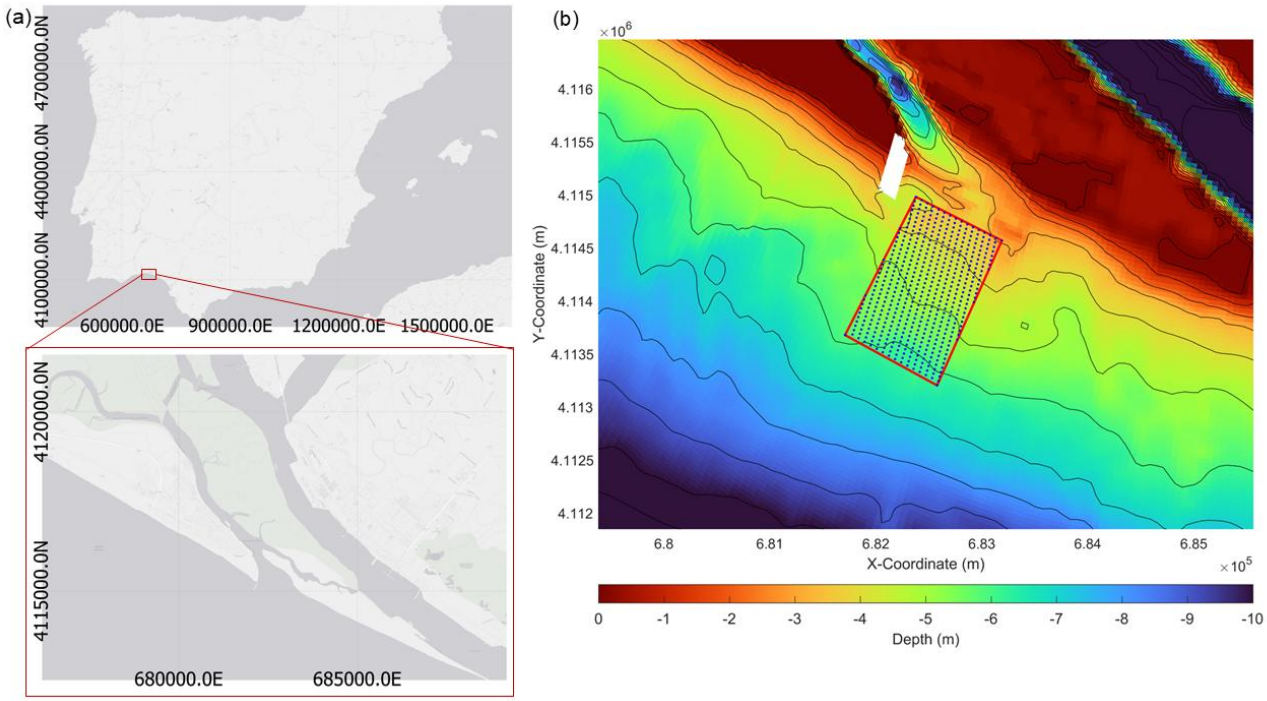

Figure 1. (a) Study area location in the Iberian Peninsula. (b) Control volume for the Punta Umbría Inlet shown on the actual bathymetry of the area. Bathymetric contours are represented every 1m, from 0 to -12 m MSL.

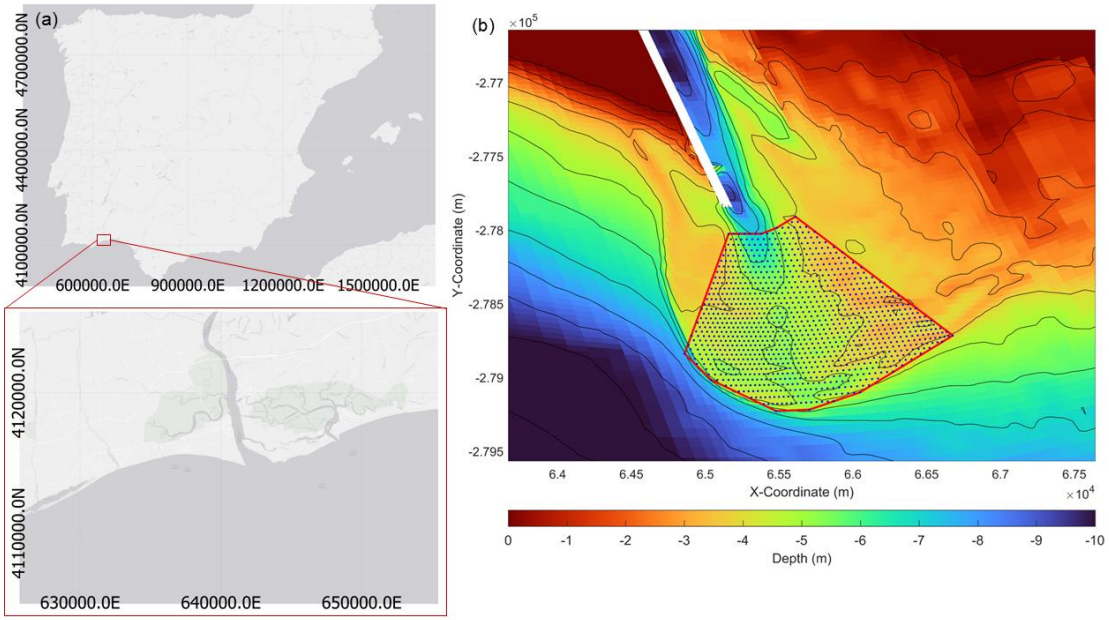

Figure 2. (a) Study area location in the Iberian Peninsula. (b) Control volume for the Guadiana Estuary shown on the actual bathymetry of the area. Bathymetric contours are represented every 1 m, from 0 to -12 m MSL.

2. **The study suggests that the optimal parameter combination (e.g., the 95th percentile threshold) may be site-specific, which is a key limitation. It is recommended that the authors include a discussion on sensitivity analysis—for example, exploring how the identification performance of this parameter set would change if key model parameters (such as bottom friction coefficient) were varied within reasonable ranges.**

Following the reviewers' recommendation, eight new simulations were conducted as a sensitivity analysis. Maintaining all other parameters constant, the uniform horizontal eddy viscosity (originally set to 2 m²/s) was tested at values of 1 and 5 m²/s. Additionally, two Chèzy roughness coefficients (60 and 70) were evaluated against the original value of 65. These four sensitivity scenarios were performed for two different experiments from the original study: (1) 1980–1981 and (3) 1999–2000.

After applying the methodology proposed in the paper, the matches obtained for the Traditional POT combination (T-POT, POT(95, 3, 12)) and the Optimal POT combination POT(95, 4, 6) were compared (Table 2). The results yielded identical match percentages in all cases, demonstrating the robustness of the model and the stability of the optimal parameters.

This information has been added to the Section 2.4 "Model setup and experimental design" in the revised manuscript, and the corresponding table has been included in the Supplementary Material (Table S4, Table 1 from the present document). The text included reads as follows: "*A sensitivity analysis was conducted through eight additional simulations to assess the robustness of the methodology with respect to key model parameters. While maintaining all other parameters constant, the uniform horizontal eddy viscosity was tested at values of 1 and 5 m²/s, and two Chèzy roughness coefficients (60 and 70, in both directions) were evaluated for comparison with the original values. These four sensitivity scenarios were performed for two representative experiments (1980–1981 and 1999–2000). The match percentages obtained for both the T-POT and the optimal POT combination*

were identical across all sensitivity scenarios (Table S4), confirming that the identified optimal parameter combination is independent of these numerical settings."

Table 1. Match results obtained for the T-POT (POT(95,3,12)) and the Optimal POT combination (POT(95,4,6)), including the original simulation and sensitivity analyses of uniform horizontal eddy viscosity (ε) and Chèzy roughness coefficients.

			LWP-ME90		Hs-ME90		LWP-ME95		Hs-ME95	
			NCV	SCV	NCV	SCV	NCV	SCV	NCV	SCV
1980-1981	T-POT	**Original**	**49.4**	**55.8**	**34.1**	**32**	**65.5**	**82.5**	**53.4**	**55.6**
		ε=1	49.4	55.8	34.1	32	65.5	82.5	53.4	55.6
		ε=5	49.4	55.8	34.1	32	65.5	82.5	53.4	55.6
		Chèzy=60	49.4	55.8	34.1	32	65.5	82.5	53.4	55.6
		Chèzy=70	49.4	55.8	34.1	32	65.5	82.5	53.4	55.6
	Optimal POT combination	**Original**	**53.2**	**55.8**	**37.1**	**35.5**	**72.9**	**82.9**	**53.4**	**62.6**
		ε=1	53.2	55.8	37.1	35.5	72.9	82.5	53.4	62.6
		ε=5	53.2	55.8	37.1	35.5	72.9	82.5	53.4	62.6
		Chèzy=60	53.2	55.8	37.1	35.5	72.9	82.5	53.4	62.6
		Chèzy=70	53.2	55.8	37.1	35.5	72.9	82.5	53.4	62.6
1999-2000	T-POT	**Original**	**50.2**	**53.3**	**36.2**	**35**	**63**	**68.25**	**47**	**36.1**
		ε=1	50.2	53.3	36.2	35	63	68.25	47	36.1
		ε=5	50.2	53.3	36.2	35	63	68.25	47	36.1
		Chèzy=60	50.2	53.3	36.2	35	63	68.25	47	36.1
		Chèzy=70	50.2	53.3	36.2	35	63	68.25	47	36.1
	Optimal POT combination	**Original**	**53.5**	**56.7**	**51.1**	**48.1**	**66.5**	**72.4**	**63.3**	**56.4**
		ε=1	53.5	56.7	51.1	48.1	66.5	72.4	63.3	56.4
		ε=5	53.5	56.7	51.1	48.1	66.5	72.4	63.3	56.4
		Chèzy=60	53.5	56.7	51.1	48.1	66.5	72.4	63.3	56.4
		Chèzy=70	53.5	56.7	51.1	48.1	66.5	72.4	63.3	56.4

3. **The use of constant river discharge and simplified tidal conditions may limit the applicability of the methodology to coasts dominated by variable riverine inputs and complex tidal dynamics. In real storm events, both factors can exhibit significant variability. The authors should address whether and how these simplifications influence the method's effectiveness in such environments.**

The authors acknowledge the referees' concerns regarding the simplified initial conditions. The use of a constant river discharge in the idealized simulations was a deliberate methodological choice, consistent with established idealized modeling frameworks in coastal morphodynamics (e.g., Jiménez-Robles et al., 2016; Ruiz-Reina & López-Ruiz, 2021). In this context, the constant discharge allows us to isolate the morphological response driven specifically by wave-induced processes, minimizing the confounding influence of fluvial forcing on the results.

However, we believe that the application of the methodology to real-world scenarios, as discussed in the previous response and in the revised manuscript, addresses these concerns. In those cases, the bathymetries reflect natural sediment variability (including spatially distributed D_{50}), and the forcing inputs are based on empirical data, including complete tidal regimes, variable river discharges, and explicit wind forcing alongside buoy-derived wave data. Furthermore, the concurrent increase in river

discharge during storm events is a physically relevant process (particularly in fluvially influenced systems such as the Guadiana estuary and the Punta Umbría Inlet) which is now explicitly accounted for in our real-world validation.

The results demonstrate that the methodology remains robust even when these additional environmental complexities are introduced. Since the effectiveness of the approach is captured in both controlled idealized cases and complex natural environments, we believe the current scope provides a comprehensive validation of its robustness.

To further clarify this point (and the related to the previous comment), we have added a discussion of these considerations in Section 6.3 (formerly Section 5.3) “Limitations and further improvements” , which now reads: *“Although the method was developed following established idealized frameworks (e.g., Jiménez-Robles et al., 2016; Ruiz-Reina & López-Ruiz, 2021), its successful validation in calibrated environments with real-world forcings, which include wind, variable river discharge, and full tidal regimes, addresses the applicability to complex coastal zones and supports the robustness of the methodology under more complex forcing conditions.”*

4. **Sediment grain size also influences coastal morphological changes. Conducting a sensitivity analysis with different sediment sizes could help broaden the applicability of the proposed method and clarify its constraints.**

The authors acknowledge the referees' concerns regarding the simplified initial conditions. Following their guidance two additional simulations were conducted as a sensitivity analysis. Using Experiment 1 (1980–1981) as a baseline, we modified the original D_{50}=1mm in the simulation to D_{50} = 0.5 mm and D_{50} = 2mm.

The results, presented in Table 2, show that the overall effectiveness of the methodology persists across different grain sizes. Specifically, a clear trend of improvement in the match related to LWP is observed in certain configurations, and the optimal POT combination consistently yields equal or higher match percentages compared to the traditional approach. Even having changes on the values according to the grain size, the overall match values are reasonably similar, with a difference that is lower than 10% for the majority of the tested conditions when referred to the original used value (D50 = 1 mm). However, given the current length of the manuscript and the addition of the new section featuring real-world data, we have decided to omit this specific information to maintain conciseness.

Table 2. Match percentages obtained for different D_{50} values during the sensitivity analysis of Experiment 1 (1980–1981).

1980-1981		LWP-ME90		Hs-ME90		LWP-ME95		Hs-ME95	
		NCV	SCV	NCV	SCV	NCV	SCV	NCV	SCV
T-POT	**Original (D_{50} = 1mm)**	**49.4**	**55.8**	**34.1**	**32**	**65.5**	**82.5**	**53.4**	**55.6**
	D_{50} = 0.5 mm	38.4	68.8	28.4	45.1	41.2	88.7	39.8	61.8
	D_{50} = 2 mm	53.3	46,47	30.8	22.3	78.2	60.3	54.7	35.8
Optimal POT combination	**Original (D_{50} = 1mm)**	**53.2**	**55. 8**	**37.1**	**35.5**	**72.9**	**82.5**	**53.4**	**62.6**
	D_{50} = 0.5 mm	38.4	68.8	31.6	49.5	41.2	88.7	39.8	69.2
	D_{50} = 2 mm	57.4	46.5	33.3	25.7	78.2	60.3	54.7	43.1

As explained above, our real-world application serves to bridge the gap between idealized modeling and complex coastal dynamics. The robustness of the methodology regarding sediment variability is further confirmed by them, which incorporate spatially distributed sediment data (see comment 1). This demonstrates that the LWP-based proxy remains effective even when subjected to the non-linearities and grain-size heterogeneity of natural coastal systems

5. **In Section 5.3 (Limitations and further improvements), limitations related to the Delft3D model configuration (e.g., neglecting wind effects, simplified initial bathymetry) are intermixed with those inherent to the LWP-based methodology itself. It is suggested that the authors clearly distinguish between limitations introduced by the numerical model and those intrinsic to the proposed LWP-POT identification method. This distinction would help readers better understand the different directions for future refinement.**

The authors appreciate this insightful comment. We agree that distinguishing between the limitations of the numerical setup (Delft3D) and those intrinsic to the LWP-based methodology is essential for future refinements.

To address the concerns regarding the numerical model's influence, we performed a new sensitivity analysis, as explained in the 2nd comment. The results demonstrate that the LWP methodology is highly robust and independent of specific numerical tuning parameters. While we acknowledge the inherent challenges associated with any numerical model, the setup used here has proven its reliability by successfully passing the sensitivity tests. Furthermore, the effectiveness of the model is confirmed by the successful calibration and validation of the real-world scenarios

Regarding the intrinsic limitations of the LWP proxy, we have introduced a physical explanation based on the Longshore vs. Cross-shore (LvC) index (López-Dóriga & Ferreira, 2017) in the discussion section 6.1 "The role of wave direction". This index quantifies whether a storm event or a coastal area is dominated by longitudinal wave energy or cross-shore processes, and reads as follows: "*Furthermore, by applying the LvC (Longshore vs. Cross-shore) index proposed by López-Dóriga and Ferreira (2017), it was found that the NCV exhibits a more cross-shore dominated in experiment 2 (1990-91) with an LvC=0.18, and in experiment 5 (2010-11) with LvC=0.01, both of which correspond to a higher H_s-match. Conversely, the SCV shows systematically higher LvC across most experiment, indicating a greater degree of longshore dominance, which corresponds with a higher LWP-match. The calculated LvC indices for all experiments and control volumes are provided in Table S5 of the Supplementary Material.*".

Table S5 of Supplementary Material corresponds to Table 3 of present document.

Table 3. LvC index calculated for each CV and for each experiment.

Year (Experiment)	NCV	SCV
1980-1981 (1)	0.25	0.30
1990-1991 (2)	0.18	0.60
1999-2000 (3)	0.85	0.66
2000-2001 (4)	0.38	0.44
2010-2011 (5)	0.01	0.40
2019-2020 (6)	0.17	0.75

Following referee's advice, some changes were made to section 6.3 of the discussion "limitations and further improvements". The new section reads as follows: "*While the methodology offers several advances, it also has specific limitations that require further refinement. The use of deep-water variables, while providing flexibility and ease of application, may introduce uncertainties when applied to complex coastal sites with intricate bathymetry or varying nearshore wave conditions. This limitation can be particularly evident in areas where wave transformation between offshore and nearshore zones is complex and nonlinear, as observed by Loureiro et al. (2012b) in their study of geologically constrained morphological variability on embayed beaches.*

The robustness of the methodology is further supported by its transition from idealized configurations to real-world scenarios (Section 5). Although the method was developed following established idealized frameworks (e.g., Jiménez-Robles et al., 2016; Ruiz-Reina & López-Ruiz, 2021), its successful validation in calibrated environments with real-world forcings, which include wind, variable river discharge, and full tidal regimes, addresses the applicability to complex coastal zones and supports the robustness of the methodology under more complex forcing conditions.

This methodological approach differs from traditional H_s-based POT techniques used in coastal engineering and opens new research directions to verify its performance under different conditions. It represents the first application of LWP-based POT, making direct comparison with traditional H_s-based POT analyses challenging. The results demonstrate that climatic events can be effectively characterized through a composite LWP-based POT analysis, incorporating established parameters such as independence criteria and event duration. While the specific parameter combination identified appears robust for the detection of morphological events in the study area, it is likely to be site-dependent, requiring site-specific calibration in future applications. Future validation efforts may become feasible as emerging monitoring technologies (e.g., continuous video systems, high-resolution remote sensing) develop the capability to provide the required temporal resolution for morphological measurements. across a wider variety of LvC conditions."

References used

García-de-Lomas, J., Payo, A., Cuesta, J. A., and Macías, D.: Morphodynamic study of a 2018 mass-stranding event at Punta Umbria Beach (Spain): Effect of Atlantic Storm Emma on Benthic Marine Organisms, J Mar Sci Eng, 7, https://doi.org/10.3390/jmse7100344, 2019.

Jiménez-Robles, A. M., Ortega-Sánchez, M., and Losada, M. A.: Effects of basin bottom slope on jet hydrodynamics and river mouth bar formation, J Geophys Res Earth Surf, 121, 1110–1133, https://doi.org/10.1002/2016JF003871, 2016.

López-Dóriga, U. and Ferreira, Ó.: Longshore and cross-shore morphological variability of a berm-bar system under low to moderate wave energy, J Coast Res, 33, 1161–1171, https://doi.org/10.2112/JCOASTRES-D-16-00050.1, 2017.

Málvarez, G., Ferreira, O., Navas, F., Cooper, J. A. G., Gracia-Prieto, F. J., and Talavera, L.: Storm impacts on a coupled human-natural coastal system: Resilience of developed coasts, Sci. Total Environ., 768, 144987, https://doi.org/10.1016/j.scitotenv.2021.144987, 2021.

Ruiz-Reina, A. and López-Ruiz, A.: Short-term river mouth bar development during extreme river discharge events: The role of the phase difference between the peak discharge and the tidal level, Coastal Engineering, 170, 103982, https://doi.org/10.1016/j.coastaleng.2021.103982, 2021.